IC at IC: IceCube can constrain the intrinsic charm of the proton

Ranjan Laha[1] and Stanley J. Brodsky[2]

[1]*Kavli Institute for Particle Astrophysics and Cosmology (KIPAC),*
Department of Physics, Stanford University, Stanford, CA 94035, USA
SLAC National Accelerator Laboratory, Menlo Park, CA 94025, USA
[2]*SLAC National Accelerator Laboratory, Stanford University, Stanford, CA 94025, USA*
rlaha@stanford.edu,sjbth@slac.stanford.edu
(Dated: August 7, 2016)

The discovery of extraterrestrial neutrinos in the ~ 30 TeV – PeV energy range by IceCube provides new constraints on high energy astrophysics. An important background to the signal are the prompt neutrinos which originate from the decay of charm hadrons produced by high energy cosmic-ray particles interacting in the Earth's atmosphere. It is conventional to use pQCD calculations of charm hadroproduction based on gluon splitting $g \to c\bar{c}$ alone. However, QCD predicts an additional "intrinsic" component of the heavy quark distribution which arises from diagrams where heavy quarks are multiply connected to the proton's valence quarks. We estimate the prompt neutrino spectrum due to intrinsic charm. We find that the atmospheric prompt neutrino flux from intrinsic charm is comparable to the pQCD contribution once we normalize the intrinsic charm differential cross sections to the ISR and the LEBC-MPS collaboration data. In future, IceCube will constrain the intrinsic charm content of the proton and will contribute to one of the major uncertainties in high energy physics phenomenology.

Introduction: Astrophysical neutrinos ($\equiv \nu + \bar{\nu}$) discovered by IceCube provide new insights on profound astrophysics and particle physics questions [1–7]. Many astrophysical models have been proposed to explain these events [8–30] and to constrain various processes [31–52]. These have spurred development of new signatures such as the through-going tracks caused by τ leptons [22] and the echo technique [53].

IceCube has detected an excess of neutrinos over the atmospheric neutrino background; however: how well do we know the background? The contribution of conventional atmospheric neutrinos, produced from the decays of π's and K's, is known to $\lesssim 10\%$ precision [54, 55]. The major background uncertainty comes from $pp \to cX$, which results in prompt neutrinos produced from the decay of charm hadrons [56–79]. The flavor ratio of prompt neutrinos is $\nu_e : \nu_\mu : \nu_\tau \approx 1 : 1 : 0.1$, and $\nu : \bar{\nu} = 1 : 1$.

Most calculations of the prompt neutrino spectrum from charm hadroproduction are based on perturbative QCD (pQCD) gluon splitting $g \to c\bar{c}$ alone [58–66, 68–76, 80]. Inclusion of nonperturbative effects, for e.g., intrinsic charm, have received much less consideration [56, 57]. Recently attention has been drawn to this issue by Refs. [78, 79]. We calculate this component by using improved theoretical and experimental input.

The important distinction between intrinsic charm and gluon splitting is that intrinsic charm uses the incoming proton energy much more efficiently due to its harder $d\sigma/dx_F$ distribution. Inclusion of the nonperturbative effects are important since the amount of intrinsic charm is an important uncertainty in QCD simulations. Due to its inherent non-perturbative nature, it has not yet been calculated from first principles, and thus its normalization must be inferred from experiment. Experiments have not yet decisively measured the normalization of intrinsic charm in the proton, which typically dominates the differential cross section at $x_F \gtrsim 0.4$.

Various experimental techniques have been suggested for measuring atmospheric prompt neutrinos [81–84]. These studies illustrate how measurements can constrain the underlying QCD mechanism in regions of the parameter space where it is difficult to obtain constraints from colliders [75].

IceCube compares the prompt neutrino spectrum derived by Enberg, Reno and Sarcevic (with modifications by Gaisser) (ERS w/G) [64, 65, 77] with their data. The present upper limits on the prompt neutrinos are near the nominal predictions [6, 85]. An additional contribution to the prompt neutrino spectrum can change the interpretation of the astrophysical neutrinos.

In this paper, we calculate the prompt neutrino contribution from intrinsic charm after normalizing the differential cross section to the ISR and the LEBC-MPS collaboration data [86, 87]. This contribution must be added to the $g \to c\bar{c}$ contribution to obtain the total atmospheric prompt neutrino spectrum. We show that the prompt neutrino flux from intrinsic charm is comparable to the pQCD contribution. The inclusion of this component as a background in the atmospheric neutrino flux can have important implications on the flux and spectral shape of the "IceCube excess neutrinos".

IceCube sensitivity is in the ball-park of the neutrino flux due to intrinsic charm [88, 89]. We emphasize that IceCube can test these differential cross sections which have proven to be difficult to measure in colliders. This synergy between IceCube and the collider searches [90–93] can constrain the normalization of the intrinsic charm contribution and solve a ~ 36 year old puzzle in QCD.

The case for Intrinsic Charm: QCD predicts two distinct contributions to the heavy quark distributions in light hadrons such as the proton. The primary contribution comes from gluon splitting $g \to Q\bar{Q}$ – the mechanism incorporated into the DGLAP pQCD evolution of structure functions. The resulting heavy-quark distribution falls as a power of $1 - x$ faster than the gluon distribution, and it is thus only important at low momentum fraction x.

A second contribution to the charm distribution $c(x, Q^2)$, which dominates at high x, comes from QCD diagrams in which the heavy quark pair is attached by two or more gluons to the valence quarks of the proton; it thus depends on the nonperturbative intrinsic structure of the proton [88, 94]. A typical intrinsic contribution comes from the $Q\bar{Q}$ cut of the hadron self-energy diagrams analogous to light-by-light diagrams. One can use the operator product expansion to show that the resulting $Q\bar{Q}$ probability $P_{Q\bar{Q}}$ falls as $1/M_Q^2$, in contrast to the $1/M_\ell^4$ behavior in Abelian QED [95, 96].

The intrinsic charm distribution in the charm structure function of the proton is thus associated with the five-quark Fock state $|uudc\bar{c} >$ of its light front wavefunction defined at fixed light-front time $\tau = t + z/c$ in the frame-independent eigensolution of the QCD Light-Front Hamiltonian. The probability distribution in invariant mass $dP_{Q\bar{Q}}/M^2$ falls as $1/M^4$ and is thus maximal in the proton light front wavefunction at minimum off-shellness [94, 96]. This occurs when all of the constituents in the hadron Fock state have the same rapidity; i.e., when they are all at rest in the parent hadron's rest frame. Equal rapidity implies that the quark's light-front momentum $x = k^+/P^+$ is proportional to its transverse mass: $x_q = (m_q^2 + k_\perp^2)/(\sum_{i=1}^{5} m_q^2 + k_\perp^2)$. Thus the heavy quarks carry most of the LF momentum of the proton. This key feature is incorporated by the BHPS model [88, 95] for the intrinsic charm contribution to the $c(x, Q^2)$ and other heavy quark distributions.

There are extensive indications for charm production at high x, beginning with the EMC measurement of $c(x, Q^2)$ in deep inelastic muon scattering [97]. The rate observed by EMC is approximately 30 times higher at $x = 0.42, Q^2 = 75$ GeV^2 than predicted by gluon splitting [98]. Intrinsic charm also predicts the observed features of the data for $\frac{d\sigma}{dx_F}(pp \to \Lambda_c X)$ as observed in ISR experiments [86] and more recently by SELEX [99]. In this case the comoving c, u and d coalesce to produce the Λ_c at high x_F where $x_F = x_c + x_u + x_d$. Similarly, the c and $\bar{c}$ can coalesce to produce the J/ψ at high x_F [100]. The production of two J/ψ at high x_F in the $\pi p \to J/\psi J/\psi X$ interaction as observed by NA3 [101], as well as the hadroproduction of double-charm baryons at high x_F, as observed by SELEX [102] corresponds to the materialization of the $|qqqc\bar{c}c\bar{c} >$, and $|q\bar{q}c\bar{c}c\bar{c} >$ Fock states of the incident hadrons [103, 104]. Although there

are large error bars, data from LEBC-MPS collaboration at 800 GeV at high x_F ($x_F \gtrsim 0.1$) on $D/\bar{D}$ production do not fall off as steeply as predicted in pQCD — the flattening tendency hints at an intrinsic charm contribution.

Other high x_F charm particle hadroproduction results are reviewed in Ref. [105]. None of these observations can be explained by the "color-drag" model used in the Pythia simulations. The corresponding $|uudb\bar{b} >$ intrinsic bottom heavy-quark Fock state can account for the observation of $pp \to \Lambda_b X$ at high x_F at the ISR [106]. The presence of charm at high x in the proton structure function is also indicated by the anomalously large $p\bar{p} \to \gamma c X$ rate reported by the D0 experiment at the Tevatron [107, 108].

An important test of $c(x, Q^2)$ at high x can be performed at the LHC by measuring the production of the Z^0 boson at high p_T, balanced by a charm jet: $pp \to Z^0 + cX$ [92, 93]. Intrinsic heavy quark distributions also lead to the production of the Higgs at high x_F at the LHC [109]. There are also proposals to perform a fixed target experiment at the LHC which will perfom high x_F studies [110]. Recent reviews and global analysis of intrinsic charm collider phenomenology are given in Refs. [89, 111–114].

Although there have been proposals to test intrinsic charm in LHC, it has not yet been demonstrated to work in practise. More ways to test this important and uncertain component of QCD are needed. We introduce the concept that IceCube can make substantial progress in increasing our knowledge about this component of QCD.

Calculations of neutrino fluxes: The earliest prompt neutrino calculations employed a proton-only cosmic ray flux known as the "broken power-law" [57, 58, 64, 115, 116]. Recent observations of cosmic ray flux indicate a mixed composition [117–119]: the Gaisser 2012 fit [117] with (i) the third component being proton (H3P), or (ii) mixed (H3A), and the Stanev et al., 2014 fit [119] fit with (iii) three (H14A), or (iv) four cosmic ray populations (H14B). We convert these to an equivalent all-proton flux, $\phi_p(E, X)$, where E and X denote the proton energy and the atmospheric column depth, respectively [70].

Assuming that the fluxes are separable in energy and column depth, we write the cascade equations as [57, 58, 64, 70, 72, 120, 121]

$$\frac{d\phi_p(E, X)}{dX} = -\frac{\phi_p(E, X)}{\lambda_p(E)} + Z_{pp}(E)\frac{\phi_p(E, X)}{\lambda_p(E)}, \quad (1)$$

$$\frac{d\phi_m(E, X)}{dX} = -\frac{\phi_m(E, X)}{\rho(X)\,\delta_m(E)} - \frac{\phi_m(E, X)}{\lambda_m(E)}$$
$$+ Z_{mm}(E)\frac{\phi_m(E, X)}{\lambda_m(E)} + Z_{pm}(E)\frac{\phi_p(E, X)}{\lambda_p(E)}, \quad (2)$$
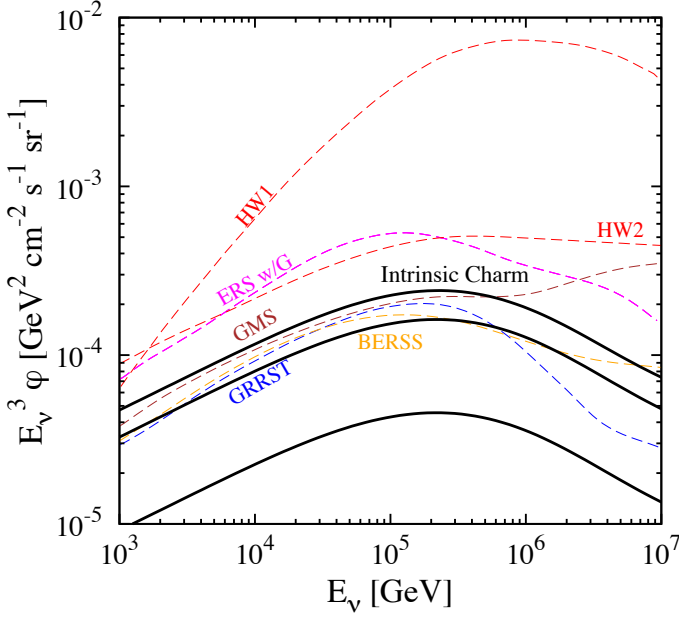
FIG. 1. Predictions for the atmospheric prompt neutrino ($\nu_e + \bar{\nu}_e$ or $\nu_\mu + \bar{\nu}_\mu$) spectrum, φ, as a function of the neutrino energy E_ν using the H3A cosmic ray input flux. We show (i) GRRST [70], (ii) BERSS [69], (iii) GMS [72], (iv) ERS w/G [64, 65], (v) HW1 [78], (vi) HW2 [79], and (vii) our calculation (Intrinsic Charm). The highest, intermediate, and the lowest flux from the intrinsic charm contribution correspond to Case (A), Case (B), and Case (C) respectively. See text for details. The upper limit from the IceCube data on the prompt neutrino flux is 1.06 times the ERS w/G flux [7].

$$\frac{d\phi_\ell(E, X)}{dX} = \sum_m Z_{m\ell}(E) \frac{\phi_m(E, X)}{\rho(X)\, \delta_m(E)}\,, \qquad (3)$$

where $\lambda_p(E)$ $[\lambda_m(E)]$ denotes the nucleon [charm hadron] attenuation length. The charm hadron flux [lepton flux from the decay of charm hadron] are denoted by $\phi_m(E, X)$ $[\phi_\ell(E, X)]$. The atmospheric density and charm hadron decay length is denoted by $\rho(X)$ and $\delta_m(E)$, respectively. The sum includes the contribution of all the relevant charm hadrons.

The production moments $Z_{pp}(E)$, $Z_{mm}(E)$, and $Z_{pm}(E)$ are defined as [58]

$$Z_{kj}(E) = \int_0^1 \frac{dx_E}{x_E} \frac{\phi_k\left(\frac{E}{x_E}, 0\right)}{\phi_k(E, 0)} \frac{\lambda_k(E)}{\lambda_k\left(\frac{E}{x_E}\right)} \frac{dn_{kj}}{dx_E}(E/x_E)\,, (4)$$

where $x_E = E/E_k$, and $dn_{kj}(E/x_E)/dx_E$ denote the production spectrum of j from the interaction of k with the air nucleon. The decay moments $Z_{m\ell}(E)$ are calculated following Refs. [58, 64, 70].

For $\lambda_p(E)$, we take the mean atomic number of air molecules, $\langle A \rangle = 14.5$. For the proton - air cross section, we take the values from QGSJet0.1c [122]. Additional

parameters required to calculate $Z_{pp}(E)$, $Z_{mm}(E)$ and $\lambda_m(E)$ are taken from Refs. [58, 69].

The calculation of $Z_{pm}(E)$ involves the differential cross section $\frac{d\sigma}{dx_F}(pp \to cX)$. There are substantial uncertainties in this differential cross section, especially at high x_F. Modern colliders are not capable of measuring this differential cross section in the forward region (high x_F) [75]. State of the art calculations, which incorporate various different constraints, are also lacking for these differential cross sections at high x_F. Taking these uncertainties into account, we adopt three test cases using the data presented by the ISR experiments and the LEBC-MPS collaboration.

Case (A): For Λ_c production, we use Ref. [124] which normalizes their differential cross section to the ISR data [86]. For D mesons, we use the shape of the differential cross sections as calculated in Ref. [125], and normalize them to the data at the highest x_F ($d\sigma/dx_F \approx 17^{+18}_{-9}$ μb at $x_F \approx 0.32$) as measured by the LEBC-MPS collaboration [87]. This measurement is within the predictions by pQCD $g \to c\bar{c}$ contribution (≈ 10 μb at $x_F = 0.32$) as estimated in Ref. [69]. However we can use the error bars in this measurement to find an allowed intrinsic charm cross section $d\sigma/dx_F \approx 25$ μb at $x_F \approx 0.32$. This corresponds to the best-fit + 1σ measurement from LEBC-MPS collaboration [87] and sets the normalization of D mesons.

Case (B): We use the charm hadron differential cross section spectral shapes as derived by Ref. [125]. To normalize these, we assume that the intrinsic charm cross section $d\sigma/dx_F \approx 25$ μb at $x_F \approx 0.32$ for the D mesons. Since we are using the same model for the D mesons and the Λ_c production, this also gives the normalization of the Λ_c.

Case (C): We again use the charm hadron differential cross section spectral shape as derived by Ref. [125]. We normalize the cross section such that the intrinsic charm cross section $d\sigma/dx_F \approx 7$ μb at $x_F \approx 0.32$ for the D mesons. This corresponds to the best fit point of the LEBC-MPS measurement.

We illustrate the uncertainty of the intrinsic charm flux by the three cases as mentioned above. The Case (C) does not represent a lower limit to the intrinsic charm contribution to the differential cross section. It is possible that the intrinsic charm contribution is lower, and this will correspond to a lower contribution to the atmospheric prompt neutrino flux compared to what is presented here. As is evident from our discussion, the intrinsic charm cross section is not at all well known. Despite decades of effort, colliders have not yet been able to definitively measure its normalization. We introduce and examine the role of IceCube in this search.

The intrinsic charm cross section scales with the mass number, A, approximately as $A^{0.755 \pm 0.016}$ according to Ref. [126]. The energy dependence of the intrinsic charm
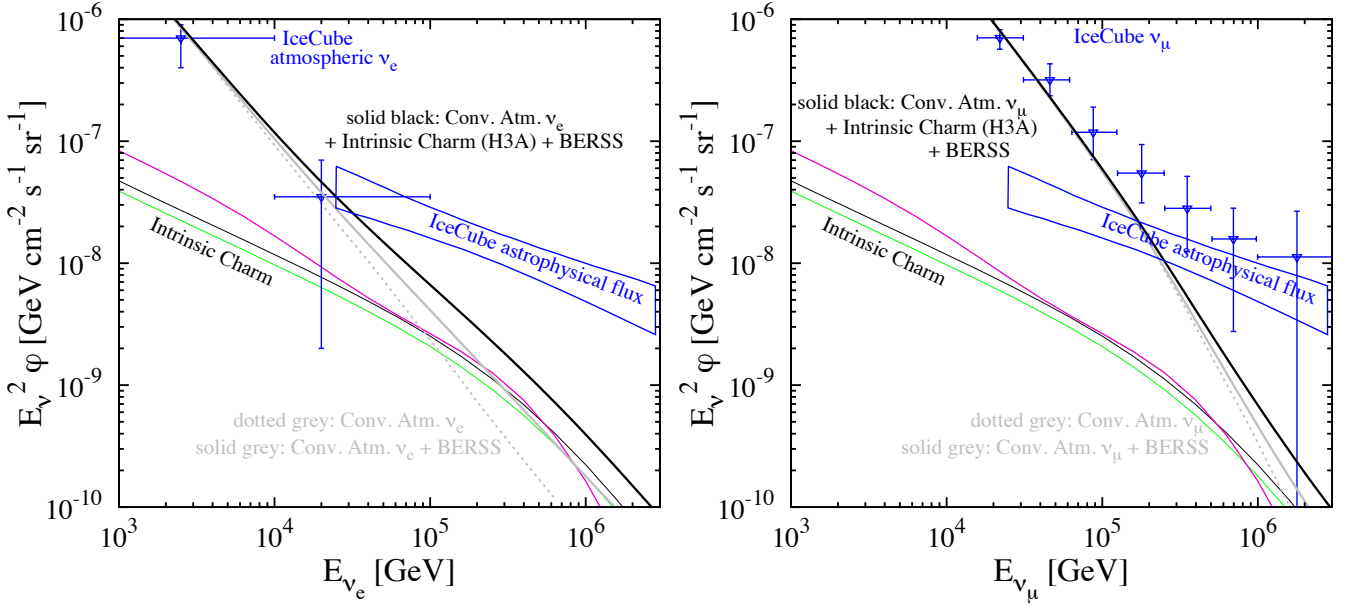
FIG. 2. **Left:** Comparison of the total atmospheric $\nu_e + \bar{\nu}_e$ data (IceCube-86 for 332 days) with calculations. The contribution to the $\nu_e + \bar{\nu}_e$ flux from intrinsic charm for Case (A) for various cosmic ray spectra is shown by the dashed lines (H3A = magenta, H3P = green, H14A = brown, and H14B = magenta. H14A and H14B are on top of each other). The conventional $\nu_e + \bar{\nu}_e$ flux [123], conventional $\nu_e + \bar{\nu}_e$ + BERSS (H3A), and conventional $\nu_e + \bar{\nu}_e$ + BERSS + intrinsic charm contribution for H3A are shown. **Right:** Same as the left panel, but for $\nu_\mu + \bar{\nu}_\mu$ [6] (IceCube-79/ 86 for 2 years). This measurement also includes the astrophysical neutrino flux. The astrophysical flux shown in these panels is from Refs. [4].

contribution follows the inelastic cross section [127].

We solve Eqs. 1 – 3 separately in the low and high energy regime [57, 58, 64, 70, 72]. The final prompt neutrino flux is a geometric interpolation of the low and high energy solutions and includes the contribution of all the charm hadrons, $D^0, \bar{D}^0, D^\pm, D_s^\pm, \Lambda_c^+$.

Our calculation improves over the previous estimates [56, 57, 78–80] in various important ways. We normalize our calculations to the ISR and the LEBC-MPS collaboration data [86, 87], which were not used in the earliest works. We employ the latest cosmic ray flux measurement, and the experimentally measured nuclear scaling of the cross section, and a theoretically motivated energy dependence of the cross section. We use a more updated calculation of the intrinsic charm cross section which takes into account the inherent non-perturbativeness of the process [124, 125] whereas some of these earlier works [78, 79] used a modified pQCD prescription to account for the high x_F data.

Results: Our predictions for the flux of neutrinos ($\nu_\mu + \bar{\nu}_\mu$ or $\nu_e + \bar{\nu}_e$) are shown in Fig. 1. The highest, intermediate and the lowest flux are given by Case (A), Case (B), and Case (C) respectively. We also show the flux calculated by BERSS [69], GMS [72], GRRST [70], HW1 [78], HW2 [79], and ERS w/G [6, 85]. Due to the uncertainties in parametrizing the $g \to c\bar{c}$ contribution, the resulting neutrino flux has an uncertainty of a factor of ~ 5 [70].

Remarkably, we find that the atmospheric prompt neutrino flux due to intrinsic charm is at the same level as the pQCD contribution.

The neutrino fluxes due to intrinsic charm are large enough to be detectable by IceCube. If IceCube does not detect atmospheric prompt neutrinos at these flux levels, then it will imply strong constraints on the intrinsic charm content of the proton.

In the intrinsic charm picture, the proton preferentially forms a charm hadron with a similar energy. In the $g \to c\bar{c}$ picture, due to its steeply falling $d\sigma/dx$ distribution, the charm hadron comes dominantly from a proton at much higher energy. A rapid energy dependence, disfavored by Refs. [124, 125], is used in Ref. [78], and this results in a much higher neutrino flux. Our results are slightly lower than the calculation presented in Ref. [79] due to the above mentioned refinements.

So far, IceCube has presented upper bounds on prompt neutrinos. IceCube assumes that the prompt neutrino flux is the ERS w/G spectrum and varies the normalization. IceCube takes into account the muon veto for downgoing events via a likelihood analysis. The present limit on the prompt neutrino spectrum is 1.06 times the ERS w/G flux [7]. These IceCube limits are close to the intrinsic charm prompt neutrino spectrum predictions, implying that IceCube can give information about intrinsic charm content of the proton in the near future.

In Fig. 2 (left), we compare our calculation for Case (A) and the measurement of the atmospheric ν_e flux [123].

The conventional atmospheric $\nu_e + \bar{\nu}_e$ flux (angular averaged) is taken from Refs. [54, 55, 123]. The conventional atmospheric ν_e + BERSS flux, the prompt ν_e flux due to intrinsic charm in case (A) for various different input cosmic ray model, the total atmospheric ν_e flux including the BERSS and due to intrinsic charm in case (A) for the H3A cosmic ray input model are also shown. We also show the astrophysical neutrino spectrum from Ref. [4] in the energy range [25 TeV, 2.8 PeV]. This shows that although the inclusion of the intrinsic charm component can change the background for astrophysical neutrinos, yet atmospheric prompt neutrinos cannot explain the "IceCube excess neutrinos".

Normalizing to the ISR and the LEBC-MPS collaboration data does not contradict the atmospheric ν_e measurements. The importance of atmospheric ν_e measurement for prompt neutrinos was pointed out in Ref. [82], and we argue that it might be the best channel to search for intrinsic charm as well. We predict that the atmospheric $\nu_e + \bar{\nu}_e$ flux due to intrinsic charm is larger than $g \to c\bar{c}$ contribution at $\gtrsim 50$ TeV. A more precise measurement of the atmospheric ν_e spectrum at slightly higher energies can give strong constraints on the intrinsic charm content of the proton.

Atmospheric prompt neutrinos cannot explain the "IceCube excess neutrinos" since prompt neutrinos have a softer spectral shape and have accompanying muons. The "IceCube excess neutrinos" have an energy spectrum varying within $\sim E^{-2.2}$ and $E^{-2.6}$ between ~ 30 TeV and 3 PeV and do not have any accompanying muons. The prompt neutrino flux follows the much softer cosmic ray spectrum.

For downgoing events, the atmospheric veto can discriminate between atmospheric and astrophysical neutrinos [128, 129]. Every atmospheric neutrino is accompanied by a muon or an electromagnetic shower from the same interaction producing the neutrino. The muon or the shower detected in coincidence with the neutrino, reduces the atmospheric neutrino flux by a factor $\gtrsim 2$ at energies $\gtrsim 10$ TeV [3]. This also results in a difference in the zenith angle distributions of astrophysical and prompt neutrinos.

The angular distribution of atmospheric prompt neutrinos is approximately isotropic at $\lesssim 10^7$ GeV. Conventional atmospheric neutrinos have a smaller vertical flux compared to the horizontal flux. Searching for atmospheric neutrinos in the vertical direction can more easily find the prompt component. More theoretical and experimental work is also required to narrow down the uncertainties of the pQCD contribution to extract the contribution of intrinsic charm from the IceCube data.

A comparison of the $\nu_\mu + \bar{\nu}_\mu$ flux from the Northern Hemisphere with calculations is shown Fig. 2 (right) [6]. The intrinsic charm component is shown for Case (A). The astrophysical neutrino spectrum in the energy range [25 TeV, 2.8 PeV] from Ref. [4] is shown. The neutrino flux due to intrinsic charm cannot increase, since it will be in contradiction with the ISR and the LEBC-MPS collaboration data. The inclusion of this contribution may result in a revision of the astrophysical neutrino spectrum. Since these events are up-going, the atmospheric veto does not play any role, and one needs to model the astrophysical neutrino flux before inferring the prompt neutrino contribution using this detection channel.

Conclusions: The landmark discovery of astrophysical neutrinos by IceCube opens up a new era. Due to the atmospheric veto employed by IceCube, any atmospheric neutrino spectrum shows an up v/s down asymmetry. The excess of neutrinos unveiled by IceCube is isotropic implying the astrophysical origin of these events. Careful consideration of the atmospheric neutrino background will impact the astrophysical neutrino flux interpretation.

The neutrino backgrounds considered so far by IceCube are the conventional atmospheric and prompt neutrinos predicted by $g \to c\bar{c}$. Intrinsic charm, rigorously predicted by QCD, has strong theoretical justification and experimental indications. We find that this often neglected component can be as large as the component due to pQCD $g \to c\bar{c}$ without violating any direct experimental constraints. This has important implications in interpreting the astrophysical neutrino flux, and inferring the atmospheric prompt neutrino component.

We present our calculation of the neutrino flux due to intrinsic charm in Fig. 1 after normalizing to the ISR and the LEBC-MPS collaboration data. We show the atmospheric prompt neutrino flux due to three different scenarios. The atmospheric prompt neutrino flux due to intrinsic charm is comparable to that due to pQCD. Our calculation is lower than Refs. [78, 79] as we use improved theoretical and experimental input.

The measurement of atmospheric $\nu_e + \bar{\nu}_e$ at higher energies is the most promising channel to discover prompt neutrinos and constrain the intrinsic charm of the proton (Fig. 2 left). The comparison of the total atmospheric flux with the $\nu_\mu + \bar{\nu}_\mu$ data, including the intrinsic charm contribution, is shown in Fig. 2 (right). The total atmospheric neutrino flux including intrinsic charm can dominate the pQCD contribution at energies $\gtrsim 200$ TeV and $\gtrsim 2$ PeV for $\nu_e + \bar{\nu}_e$ and $\nu_\mu + \bar{\nu}_\mu$ respectively.

The conventional atmospheric $\nu_e + \bar{\nu}_e$ flux is lower, implying that the prompt component is more visible in this channel. We estimate that a measurement of the atmospheric $\nu_e + \bar{\nu}_e$ flux at ~ 200 TeV at $\sim 50\%$ accuracy will cleanly distinguish between the pQCD and intrinsic charm component.

The current upper limit on prompt neutrinos is 1.06 times the ERS w/G flux. The neutrino flux due to intrinsic charm is at the same level as the ERS w/G flux implying that IceCube can constrain intrinsic charm of the proton. This shows that IceCube can constrain QCD

predictions in regions of parameter space which have been difficult to constrain in colliders for decades.

The multi-pronged approach consisting of IceCube data, collider physics, and global analysis will help us constrain the intrinsic charm of the proton, and solve a ~ 36 year old problem in QCD. The use of neutrinos, a weakly interacting particle, to constrain the strong interactions will also highlight the importance of cross disciplinary searches in physics.

[1] **IceCube** Collaboration, M. G. Aartsen *et al.*, "First observation of PeV-energy neutrinos with IceCube", *Phys. Rev. Lett.* **111** (2013) 021103, arXiv:1304.5356.

[2] **IceCube** Collaboration, M. G. Aartsen *et al.*, "Evidence for High-Energy Extraterrestrial Neutrinos at the IceCube Detector", *Science* **342** (2013) 1242856, arXiv:1311.5238.

[3] **IceCube** Collaboration, M. G. Aartsen *et al.*, "Observation of High-Energy Astrophysical Neutrinos in Three Years of IceCube Data", *Phys. Rev. Lett.* **113** (2014) 101101, arXiv:1405.5303.

[4] **IceCube** Collaboration, M. G. Aartsen *et al.*, "A combined maximum-likelihood analysis of the high-energy astrophysical neutrino flux measured with IceCube", *Astrophys. J.* **809** (2015), no. 1, 98, arXiv:1507.03991.

[5] **IceCube** Collaboration, M. G. Aartsen *et al.*, "Evidence for Astrophysical Muon Neutrinos from the Northern Sky with IceCube", *Phys. Rev. Lett.* **115** (2015), no. 8, 081102, arXiv:1507.04005.

[6] **IceCube** Collaboration, M. G. Aartsen *et al.*, "The IceCube Neutrino Observatory - Contributions to ICRC 2015 Part II: Atmospheric and Astrophysical Diffuse Neutrino Searches of All Flavors", in "Proceedings, 34th International Cosmic Ray Conference (ICRC 2015)". 2015. arXiv:1510.05223.

[7] **IceCube** Collaboration, M. G. Aartsen *et al.*, "Observation and Characterization of a Cosmic Muon Neutrino Flux from the Northern Hemisphere using six years of IceCube data", arXiv:1607.08006.

[8] R. Laha, J. F. Beacom, B. Dasgupta, S. Horiuchi, and K. Murase, "Demystifying the PeV Cascades in IceCube: Less (Energy) is More (Events)", *Phys. Rev.* **D88** (2013) 043009, arXiv:1306.2309.

[9] K. Murase and K. Ioka, "TeV?PeV Neutrinos from Low-Power Gamma-Ray Burst Jets inside Stars", *Phys. Rev. Lett.* **111** (2013), no. 12, 121102, arXiv:1306.2274.

[10] L. A. Anchordoqui *et al.*, "Cosmic Neutrino Pevatrons: A Brand New Pathway to Astronomy, Astrophysics, and Particle Physics", *JHEAp* **1-2** (2014) 1–30, arXiv:1312.6587.

[11] M. D. Kistler, T. Stanev, and H. Yuksel, "Cosmic PeV Neutrinos and the Sources of Ultrahigh Energy Protons", *Phys. Rev.* **D90** (2014), no. 12, 123006, arXiv:1301.1703.

[12] M. Ahlers and K. Murase, "Probing the Galactic Origin of the IceCube Excess with Gamma-Rays", *Phys. Rev.* **D90** (2014), no. 2, 023010, arXiv:1309.4077.

[13] L. A. Anchordoqui, "Neutron beta-decay as the origin of IceCube?s PeV (anti)neutrinos", *Phys. Rev.* **D91** (2015) 027301, arXiv:1411.6457.

[14] K. Fang, "High-Energy Neutrino Signatures of Newborn Pulsars In the Local Universe", *JCAP* **1506** (2015), no. 06, 004, arXiv:1411.2174.

[15] K. Kashiyama and P. Meszaros, "Galaxy Mergers as a Source of Cosmic Rays, Neutrinos, and Gamma Rays", *Astrophys. J.* **790** (2014) L14, arXiv:1405.3262.

[16] P. Baerwald, M. Bustamante, and W. Winter, "Are gamma-ray bursts the sources of ultra-high energy cosmic rays?", *Astropart. Phys.* **62** (2015) 66–91, arXiv:1401.1820.

[17] S. Ando, I. Tamborra, and F. Zandanel, "Tomographic Constraints on High-Energy Neutrinos of Hadronuclear Origin", *Phys. Rev. Lett.* **115** (2015), no. 22, 221101, arXiv:1509.02444.

[18] K. Emig, C. Lunardini, and R. Windhorst, "Do high energy astrophysical neutrinos trace star formation?", *JCAP* **1512** (2015) 029, arXiv:1507.05711.

[19] I. Tamborra and S. Ando, "Inspecting the supernova?gamma-ray-burst connection with high-energy neutrinos", *Phys. Rev.* **D93** (2016), no. 5, 053010, arXiv:1512.01559.

[20] M. D. Kistler, "Problems and Prospects from a Flood of Extragalactic TeV Neutrinos in IceCube", arXiv:1511.01530.

[21] M. D. Kistler, "On TeV Gamma Rays and the Search for Galactic Neutrinos", arXiv:1511.05199.

[22] M. D. Kistler and R. Laha, "Multi-PeV Signals from a New Astrophysical Neutrino Flux Beyond the Glashow Resonance", arXiv:1605.08781.

[23] R. Moharana and S. Razzaque, "Angular correlation between IceCube high-energy starting events and starburst sources", arXiv:1606.04420.

[24] F. Halzen and A. Kheirandish, "High Energy Neutrinos from Recent Blazar Flares", arXiv:1605.06119.

[25] G. Pagliaroli, C. Evoli, and F. L. Villante, "Expectations for high energy diffuse galactic neutrinos for different cosmic ray distributions", arXiv:1606.04489.

[26] L. A. Anchordoqui, "Neutrino lighthouse powered by Sagittarius A* disk dynamo", arXiv:1606.01816.

[27] R. K. Dey, S. Dam, and S. Ray, "Searching PeV neutrinos from photomeson interactions in magnetars", arXiv:1603.07833.

[28] K. Fang and M. C. Miller, "A New Method for Finding Point Sources in High-energy Neutrino Data", arXiv:1603.09306.

[29] A. Palladino and F. Vissani, "Extragalactic plus Galactic model for IceCube neutrino events", arXiv:1601.06678.

[30] N. Senno, K. Murase, and P. Meszaros, "Choked Jets and Low-Luminosity Gamma-Ray Bursts as Hidden Neutrino Sources", *Phys. Rev.* **D93** (2016), no. 8, 083003, arXiv:1512.08513.

[31] M. Bustamante, J. F. Beacom, and W. Winter, "Theoretically palatable flavor combinations of astrophysical neutrinos", *Phys. Rev. Lett.* **115** (2015), no. 16, 161302, arXiv:1506.02645.

[32] C. A. Arguelles, T. Katori, and J. Salvado, "New Physics in Astrophysical Neutrino Flavor", *Phys. Rev. Lett.* **115** (2015) 161303, arXiv:1506.02043.

[33] A. C. Vincent, S. Palomares-Ruiz, and O. Mena, "Analysis of the 4-year IceCube HESE data", arXiv:1605.01556.

[34] J. Kopp, J. Liu, and X.-P. Wang, "Boosted Dark Matter in IceCube and at the Galactic Center", *JHEP* **04** (2015) 105, arXiv:1503.02669.

[35] B. Dasgupta and R. Laha, "Neutrinos in IceCube/KM3NeT as probes of Dark Matter Substructures in Galaxy Clusters", *Phys. Rev.* **D86** (2012) 093001, arXiv:1206.1322.

[36] K. Murase, R. Laha, S. Ando, and M. Ahlers, "Testing the Dark Matter Scenario for PeV Neutrinos Observed in IceCube", *Phys. Rev. Lett.* **115** (2015), no. 7, 071301, arXiv:1503.04663.

[37] C. Rott, K. Kohri, and S. C. Park, "Superheavy dark matter and IceCube neutrino signals: Bounds on decaying dark matter", *Phys. Rev.* **D92** (2015), no. 2, 023529, arXiv:1408.4575.

[38] A. Esmaili, S. K. Kang, and P. D. Serpico, "IceCube events and decaying dark matter: hints and constraints", *JCAP* **1412** (2014), no. 12, 054, arXiv:1410.5979.

[39] A. Bhattacharya, M. H. Reno, and I. Sarcevic, "Reconciling neutrino flux from heavy dark matter decay and recent events at IceCube", *JHEP* **06** (2014) 110, arXiv:1403.1862.

[40] A. Bhattacharya, R. Gandhi, and A. Gupta, "The Direct Detection of Boosted Dark Matter at High Energies and PeV events at IceCube", *JCAP* **1503** (2015), no. 03, 027, arXiv:1407.3280.

[41] K. C. Y. Ng and J. F. Beacom, "Cosmic neutrino cascades from secret neutrino interactions", *Phys. Rev.* **D90** (2014), no. 6, 065035, arXiv:1404.2288, [Erratum: Phys. Rev.D90,no.8,089904(2014)].

[42] B. Dutta, Y. Gao, T. Li, C. Rott, and L. E. Strigari, "Leptoquark implication from the CMS and IceCube experiments", *Phys. Rev.* **D91** (2015) 125015, arXiv:1505.00028.

[43] P. Ko and Y. Tang, "IceCube Events from Heavy DM decays through the Right-handed Neutrino Portal", *Phys. Lett.* **B751** (2015) 81–88, arXiv:1508.02500.

[44] C. El Aisati, M. Gustafsson, T. Hambye, and T. Scarna, "Dark Matter Decay to a Photon and a Neutrino: the Double Monochromatic Smoking Gun Scenario", *Phys. Rev.* **D93** (2016), no. 4, 043535, arXiv:1510.05008.

[45] S. M. Boucenna, M. Chianese, G. Mangano, G. Miele, S. Morisi, O. Pisanti, and E. Vitagliano, "Decaying Leptophilic Dark Matter at IceCube", *JCAP* **1512** (2015), no. 12, 055, arXiv:1507.01000.

[46] S. B. Roland, B. Shakya, and J. D. Wells, "PeV neutrinos and a 3.5 keV x-ray line from a PeV-scale supersymmetric neutrino sector", *Phys. Rev.* **D92** (2015), no. 9, 095018, arXiv:1506.08195.

[47] J. F. Cherry, A. Friedland, and I. M. Shoemaker, "Short-baseline neutrino oscillations, Planck, and IceCube", arXiv:1605.06506.

[48] P. S. B. Dev, D. K. Ghosh, and W. Rodejohann, "R-parity Violating Supersymmetry at IceCube", arXiv:1605.09743.

[49] P. S. B. Dev, D. Kazanas, R. N. Mohapatra, V. L. Teplitz, and Y. Zhang, "Heavy right-handed neutrino dark matter and PeV neutrinos at IceCube", arXiv:1606.04517.

[50] Y. Ema and T. Moroi, "Early Decay of Peccei-Quinn Fermion and the IceCube Neutrino Events", arXiv:1606.04186.

[51] P. Di Bari, P. O. Ludl, and S. Palomares-Ruiz, "Unifying leptogenesis, dark matter and high-energy neutrinos with right-handed neutrino mixing via Higgs portal", arXiv:1606.06238.

[52] U. K. Dey, S. Mohanty, and G. Tomar, "Leptoquarks: 750 GeV Diphoton Resonance and IceCube Events", arXiv:1606.07903.

[53] S. W. Li, M. Bustamante, and J. F. Beacom, "Echo Technique to Distinguish Flavors of Astrophysical Neutrinos", arXiv:1606.06290.

[54] M. Honda, T. Kajita, K. Kasahara, S. Midorikawa, and T. Sanuki, "Calculation of atmospheric neutrino flux using the interaction model calibrated with atmospheric muon data", *Phys. Rev.* **D75** (2007) 043006, arXiv:astro-ph/0611418.

[55] G. D. Barr, T. K. Gaisser, P. Lipari, S. Robbins, and T. Stanev, "A Three - dimensional calculation of atmospheric neutrinos", *Phys. Rev.* **D70** (2004) 023006, arXiv:astro-ph/0403630.

[56] E. V. Bugaev, V. A. Naumov, S. I. Sinegovsky, and E. S. Zaslavskaya, "Prompt Leptons in Cosmic Rays", *Nuovo Cim.* **C12** (1989) 41–73.

[57] P. Gondolo, G. Ingelman, and M. Thunman, "Charm production and high-energy atmospheric muon and neutrino fluxes", *Astropart. Phys.* **5** (1996) 309–332, arXiv:hep-ph/9505417.

[58] L. Pasquali, M. H. Reno, and I. Sarcevic, "Lepton fluxes from atmospheric charm", *Phys. Rev.* **D59** (1999) 034020, arXiv:hep-ph/9806428.

[59] G. Gelmini, P. Gondolo, and G. Varieschi, "Prompt atmospheric neutrinos and muons: NLO versus LO QCD predictions", *Phys. Rev.* **D61** (2000) 036005, arXiv:hep-ph/9904457.

[60] G. Gelmini, P. Gondolo, and G. Varieschi, "Prompt atmospheric neutrinos and muons: Dependence on the gluon distribution function", *Phys. Rev.* **D61** (2000) 056011, arXiv:hep-ph/9905377.

[61] J. Candia and E. Roulet, "Rigidity dependent knee and cosmic ray induced high energy neutrino fluxes", *JCAP* **0309** (2003) 005, arXiv:astro-ph/0306632.

[62] A. D. Martin, M. G. Ryskin, and A. M. Stasto, "Prompt neutrinos from atmospheric $c\bar{c}$ and $b\bar{b}$ production and the gluon at very small x", *Acta Phys. Polon.* **B34** (2003) 3273–3304, arXiv:hep-ph/0302140.

[63] P. Berghaus, T. Montaruli, and J. Ranft, "Charm Production in DPMJET", *JCAP* **0806** (2008) 003, arXiv:0712.3089.

[64] R. Enberg, M. H. Reno, and I. Sarcevic, "Prompt neutrino fluxes from atmospheric charm", *Phys. Rev.* **D78** (2008) 043005, arXiv:0806.0418.

[65] T. K. Gaisser, "Atmospheric leptons", *EPJ Web Conf.* **52** (2013) 09004, arXiv:1303.1431.

[66] E.-J. Ahn, R. Engel, A. Fedynitch, T. K. Gaisser, F. Riehn, and T. Stanev, "Atmospheric neutrinos at high energy", in "Proceedings, 33rd International Cosmic Ray Conference (ICRC2013): Rio de Janeiro, Brazil, July 2-9, 2013", p. 1144.

[67] P. Lipari, "Establishing the astrophysical origin of a signal in a neutrino telescope", arXiv:1308.2086.

[68] F. Riehn, R. Engel, A. Fedynitch, T. K. Gaisser, and T. Stanev, "Charm production in SIBYLL", *EPJ Web Conf.* **99** (2015) 12001, arXiv:1502.06353.

[69] A. Bhattacharya, R. Enberg, M. H. Reno, I. Sarcevic, and A. Stasto, "Perturbative charm production and the prompt atmospheric neutrino flux in light of RHIC and LHC", *JHEP* **06** (2015) 110, arXiv:1502.01076.

[70] R. Gauld, J. Rojo, L. Rottoli, S. Sarkar, and J. Talbert, "The prompt atmospheric neutrino flux in the light of LHCb", *JHEP* **02** (2016) 130, arXiv:1511.06346.

[71] R. Gauld, J. Rojo, L. Rottoli, and J. Talbert, "Charm production in the forward region: constraints on the small-x gluon and backgrounds for neutrino astronomy", *JHEP* **11** (2015) 009, arXiv:1506.08025.

[72] M. V. Garzelli, S. Moch, and G. Sigl, "Lepton fluxes from atmospheric charm revisited", *JHEP* **10** (2015) 115, arXiv:1507.01570.

[73] A. Fedynitch, R. Engel, T. K. Gaisser, F. Riehn, and T. Stanev, "Calculation of conventional and prompt lepton fluxes at very high energy", *EPJ Web Conf.* **99** (2015) 08001, arXiv:1503.00544.

[74] A. Fedynitch, R. Engel, T. K. Gaisser, F. Riehn, and S. Todor, "MCEQ - numerical code for inclusive lepton flux calculations", *PoS* **ICRC2015** (2015) 1129.

[75] C. Baus, R. Engel, A. Fedynitch, U. Kramer, T. Pierog, F. Riehn, and R. Ulrich, "The impact of a fixed-target experiment with LHC beam for astroparticle physics", *PoS* **ICRC2015** (2015) 407.

[76] A. Bhattacharya, R. Enberg, Y. S. Jeong, C. S. Kim, M. H. Reno, I. Sarcevic, and A. Stasto, "Prompt atmospheric neutrino fluxes: perturbative QCD models and nuclear effects", arXiv:1607.00193.

[77] T. K. Gaisser, "Atmospheric Neutrinos", *J. Phys. Conf. Ser.* **718** (2016), no. 5, 052014, arXiv:1605.03073.

[78] F. Halzen and L. Wille, "Upper Limit on Forward Charm Contribution to Atmospheric Neutrino Flux", arXiv:1601.03044.

[79] F. Halzen and L. Wille, "On the Charm Contribution to the Atmospheric Neutrino Flux", arXiv:1605.01409.

[80] A. Fedynitch, "Phenomenology of atmospheric neutrinos", *EPJ Web Conf.* **116** (2016) 11010.

[81] G. Gelmini, P. Gondolo, and G. Varieschi, "Measuring the prompt atmospheric neutrino flux with down-going muons in neutrino telescopes.", *Phys. Rev.* **D67** (2003) 017301, arXiv:hep-ph/0209111.

[82] J. F. Beacom and J. Candia, "Shower power: Isolating the prompt atmospheric neutrino flux using electron neutrinos", *JCAP* **0411** (2004) 009, arXiv:hep-ph/0409046.

[83] R. Gandhi and S. Panda, "Probing the cosmic ray 'Knee' and very high energy prompt muon and neutrino fluxes via underground muons", *JCAP* **0607** (2006) 011, arXiv:hep-ph/0512179.

[84] P. Desiati and T. K. Gaisser, "Seasonal variation of atmospheric leptons as a probe of charm", *Phys. Rev. Lett.* **105** (2010) 121102, arXiv:1008.2211.

[85] **IceCube** Collaboration, M. G. Aartsen *et al.*, "Atmospheric and astrophysical neutrinos above 1 TeV interacting in IceCube", *Phys. Rev.* **D91** (2015), no. 2, 022001, arXiv:1410.1749.

[86] **R608** Collaboration, P. Chauvat *et al.*, "Production of $\Lambda(c)$ With Large X(f) at the ISR", *Phys. Lett.* **B199** (1987) 304.

[87] R. Ammar *et al.*, "D-Meson Production in 800-GeV/c p Pinteractions", *Phys. Rev. Lett.* **61** (1988) 2185–2188.

[88] S. J. Brodsky, P. Hoyer, C. Peterson, and N. Sakai, "The Intrinsic Charm of the Proton", *Phys. Lett.* **B93** (1980) 451–455.

[89] S. J. Brodsky, A. Kusina, F. Lyonnet, I. Schienbein, H. Spiesberger, and R. Vogt, "A review of the intrinsic heavy quark content of the nucleon", *Adv. High Energy Phys.* **2015** (2015) 231547, arXiv:1504.06287.

[90] S. Rostami, A. Khorramian, A. Aleedaneshvar, and M. Goharipour, "The impact of the intrinsic charm quark content of a proton on the differential $\gamma + c$ cross section", *J. Phys.* **G43** (2016), no. 5, 055001, arXiv:1510.08421.

[91] G. Bailas and V. P. Goncalves, "Phenomenological implications of the intrinsic charm in the Z boson production at the LHC", *Eur. Phys. J.* **C76** (2016), no. 3, 105, arXiv:1512.06007.

[92] T. Boettcher, P. Ilten, and M. Williams, "Direct probe of the intrinsic charm content of the proton", *Phys. Rev.* **D93** (2016), no. 7, 074008, arXiv:1512.06666.

[93] A. V. Lipatov, G. I. Lykasov, Y. Y. Stepanenko, and V. A. Bednyakov, "Probing proton intrinsic charm in photon or Z boson production accompanied by heavy jets at LHC", arXiv:1606.04882.

[94] S. J. Brodsky, J. C. Collins, S. D. Ellis, J. F. Gunion, and A. H. Mueller, "INTRINSIC CHEVROLETS AT THE SSC", in "1984 DPF Summer Study on the Design and Utilization of the Superconducting Super Collider (SSC) (Snowmass 84) Snowmass, Colo., June 23-July 13, 1984". 1984.

[95] S. J. Brodsky, C. Peterson, and N. Sakai, "Intrinsic Heavy Quark States", *Phys. Rev.* **D23** (1981) 2745.

[96] M. Franz, M. V. Polyakov, and K. Goeke, "Heavy quark mass expansion and intrinsic charm in light hadrons", *Phys. Rev.* **D62** (2000) 074024, arXiv:hep-ph/0002240.

[97] **European Muon** Collaboration, J. J. Aubert *et al.*, "Production of charmed particles in 250-GeV μ^+ - iron interactions", *Nucl. Phys.* **B213** (1983) 31–64.

[98] B. W. Harris, J. Smith, and R. Vogt, "Reanalysis of the EMC charm production data with extrinsic and intrinsic charm at NLO", *Nucl. Phys.* **B461** (1996) 181–196, arXiv:hep-ph/9508403.

[99] **SELEX** Collaboration, F. G. Garcia *et al.*, "Hadronic production of Lambda(c) from 600-GeV/c pi-, Sigma- and p beams", *Phys. Lett.* **B528** (2002) 49–57, arXiv:hep-ex/0109017.

[100] **NA3** Collaboration, J. Badier *et al.*, "Experimental J/psi Hadronic Production from 150-GeV/c to 280-GeV/c", *Z. Phys.* **C20** (1983) 101.

[101] **NA3** Collaboration, J. Badier *et al.*, "Evidence for $\psi\psi$ Production in π^- Interactions at 150-GeV/c and 280-GeV/c", *Phys. Lett.* **B114** (1982) 457–460.

[102] **SELEX** Collaboration, A. Ocherashvili *et al.*, "Confirmation of the double charm baryon Xi+(cc)(3520) via its decay to p D+ K-", *Phys. Lett.* **B628** (2005) 18–24, arXiv:hep-ex/0406033.

[103] R. Vogt and S. J. Brodsky, "Intrinsic charm contribution to double quarkonium hadroproduction", *Phys. Lett.* **B349** (1995) 569–575, arXiv:hep-ph/9503206.

[104] S. Koshkarev and V. Anikeev, "Production of the Doubly Charmed Baryons – the double intrinsic charm approach", arXiv:1605.03070.

[105] R. Vogt and S. J. Brodsky, "QCD and intrinsic heavy quark predictions for leading charm and beauty hadroproduction", *Nucl. Phys.* **B438** (1995) 261–277, arXiv:hep-ph/9405236.

[106] G. Bari *et al.*, "The Lambda/b0 beauty baryon production in proton proton interactions at s**(1/2) = 62-GeV: A Second observation", *Nuovo Cim.* **A104** (1991) 1787–1800.

[107] **D0** Collaboration, V. M. Abazov *et al.*, "Measurement of gamma + b + X and gamma + c + X production cross sections in p anti-p collisions at s**(1/2) = 1.96-TeV", *Phys. Rev. Lett.* **102** (2009) 192002, arXiv:0901.0739.

[108] C. Mesropian and D. Bandurin, "Review of physics results from the Tevatron: QCD physics", *Int. J. Mod. Phys.* **A30** (2015), no. 06, 1541002, arXiv:1409.5639.

[109] S. J. Brodsky, A. S. Goldhaber, B. Z. Kopeliovich, and I. Schmidt, "Higgs Hadroproduction at Large Feynman x", *Nucl. Phys.* **B807** (2009) 334–347, arXiv:0707.4658.

[110] S. J. Brodsky, F. Fleuret, C. Hadjidakis, and J. P. Lansberg, "Physics Opportunities of a Fixed-Target Experiment using the LHC Beams", *Phys. Rept.* **522** (2013) 239–255, arXiv:1202.6585.

[111] S. Dulat, T.-J. Hou, J. Gao, J. Huston, J. Pumplin, C. Schmidt, D. Stump, and C. P. Yuan, "Intrinsic Charm Parton Distribution Functions from CTEQ-TEA Global Analysis", *Phys. Rev.* **D89** (2014), no. 7, 073004, arXiv:1309.0025.

[112] P. Jimenez-Delgado, T. J. Hobbs, J. T. Londergan, and W. Melnitchouk, "New limits on intrinsic charm in the nucleon from global analysis of parton distributions", *Phys. Rev. Lett.* **114** (2015), no. 8, 082002, arXiv:1408.1708.

[113] S. J. Brodsky and S. Gardner, "Comment on ?New Limits on Intrinsic Charm in the Nucleon from Global Analysis of Parton Distributions?", *Phys. Rev. Lett.* **116** (2016), no. 1, 019101, arXiv:1504.00969.

[114] **NNPDF** Collaboration, R. D. Ball, V. Bertone, M. Bonvini, S. Carrazza, S. Forte, A. Guffanti, N. P. Hartland, J. Rojo, and L. Rottoli, "A Determination of the Charm Content of the Proton", arXiv:1605.06515.

[115] L. Pasquali, M. H. Reno, and I. Sarcevic, "Secondary decays in atmospheric charm contributions to the flux of muons and muon neutrinos", *Astropart. Phys.* **9** (1998) 193–202, arXiv:hep-ph/9710363.

[116] L. Pasquali and M. H. Reno, "Tau-neutrino fluxes from atmospheric charm", *Phys. Rev.* **D59** (1999) 093003, arXiv:hep-ph/9811268.

[117] T. K. Gaisser, "Spectrum of cosmic-ray nucleons, kaon production, and the atmospheric muon charge ratio", *Astropart. Phys.* **35** (2012) 801–806, arXiv:1111.6675.

[118] T. K. Gaisser, T. Stanev, and S. Tilav, "Cosmic Ray Energy Spectrum from Measurements of Air Showers", *Front. Phys. China* **8** (2013) 748–758, arXiv:1303.3565.

[119] T. Stanev, T. K. Gaisser, and S. Tilav, "High energy cosmic rays: sources and fluxes", *Nucl. Instrum. Meth.* **A742** (2014) 42–46.

[120] T. K. Gaisser, "Cosmic rays and particle physics", 1990.

[121] P. Lipari, "Lepton spectra in the earth's atmosphere", *Astropart. Phys.* **1** (1993) 195–227.

[122] N. N. Kalmykov and S. S. Ostapchenko, "The Nucleus-nucleus interaction, nuclear fragmentation, and fluctuations of extensive air showers", *Phys. Atom. Nucl.* **56** (1993) 346–353, [Yad. Fiz.56N3,105(1993)].

[123] **IceCube** Collaboration, M. G. Aartsen *et al.*, "Measurement of the Atmospheric ν_e Spectrum with IceCube", *Phys. Rev.* **D91** (2015) 122004, arXiv:1504.03753.

[124] T. J. Hobbs, J. T. Londergan, and W. Melnitchouk, "Phenomenology of nonperturbative charm in the nucleon", *Phys. Rev.* **D89** (2014), no. 7, 074008, arXiv:1311.1578.

[125] T. Gutierrez and R. Vogt, "Leading charm in hadron nucleus interactions in the intrinsic charm model", *Nucl. Phys.* **B539** (1999) 189–214, arXiv:hep-ph/9808213.

[126] **SELEX** Collaboration, A. Blanco-Covarrubias *et al.*, "Nuclear Dependence of Charm Production", *Eur. Phys. J.* **C64** (2009) 637–644, arXiv:0902.0355.

[127] G. Antchev *et al.*, "First measurement of the total proton-proton cross section at the LHC energy of $\sqrt{s}$ =7 TeV", *Europhys. Lett.* **96** (2011) 21002, arXiv:1110.1395.

[128] S. Schonert, T. K. Gaisser, E. Resconi, and O. Schulz, "Vetoing atmospheric neutrinos in a high energy neutrino telescope", *Phys. Rev.* **D79** (2009) 043009, arXiv:0812.4308.

[129] T. K. Gaisser, K. Jero, A. Karle, and J. van Santen, "Generalized self-veto probability for atmospheric neutrinos", *Phys. Rev.* **D90** (2014), no. 2, 023009, arXiv:1405.0525.
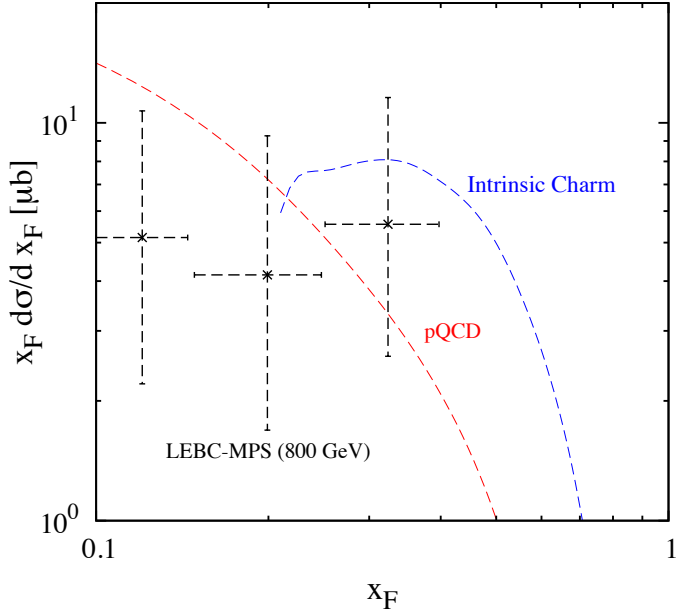
Supplemental Materials

FIG. 3. The data at $x_F \gtrsim 0.1$ as obtained by the LEBC-MPS collaboration. We compare the data points with the perturbative calculation as given in Ref. [69]. We also show the intrinsic charm differential cross section for Case (A) and (B). The differential cross section for Case (C) has the same shape, but a normalization which is $\sim 28\%$ of that shown in this figure.

In this Supplemental Material, we show the $d\sigma/dx_F$ distribution that we use in our calculations.

The data points as measured by the LEBC-MPS collaboration for $x_F \gtrsim 0.1$ is shown in the Figure. The beam energy in this fixed target experiment was 800 GeV. We also show the pQCD prediction based on Ref. [69].

Although there are large error bars, the data points hint at a flat behavior with increasing x_F. This is in contrast to the pQCD prediction which falls steeply. Given this flattening hint and the large error bars, one can postulate an intrinsic charm contribution to the differential cross section. Due to the robust theoretical prediction for intrinsic charm, we can evaluate its contribution to the LEBC-MPS kinematics. The intrinsic charm differential cross section used in this work is such that it does not exceed the best - fit + 1-sigma measurement by the LEBC-MPS collaboration. We assume that the intrinsic charm differential cross section has a negligible value below $x_F = 0.2$, and thus our result is conservative. The intrinsic charm differential cross section as shown in the figure results in a total $d\sigma/dx_F \approx 35 \, \mu$b at $x_F \approx 0.32$. This is the normalization of the intrinsic charm differential cross section that is used in Cases (A) and (B).

For Case (C) we use the same shape of the intrinsic charm differential cross section as before, but with a reduced normalization. The normalization is this case is such that the total $d\sigma/dx_F \approx 25 \, \mu$b at $x_F \approx 0.32$. The highest x_F at which a measurement has been made by the LEBC-MPS collaboration is $x_F \approx 0.32$. A future experiment which can measure the differential cross section at a higher x_F will be invaluable for this field.

Future experiment using different beam energies, and nuclear targets can deduce the energy dependence and nuclear dependence of the cross section. Such a measurement will reduce most of the uncertainties in the calculations of the prompt neutrinos flux due to intrinsic charm.